

ARTICLE

Fe₃O₄@NCs/BF_{0.2}: A magnetic bio-based nanocatalyst for the synthesis of 2,3-dihydro-1*H*-perimidines

Bi Bi Fatemeh Mirjalili  | Mahnaz Imani

Department of Chemistry, College of Science, Yazd University, Yazd, I. R. Iran

CorrespondenceBi Bi Fatemeh Mirjalili, Department of Chemistry, College of Science, Yazd University, Yazd, 89195-741, I. R. Iran.
Email: fmirjalili@yazd.ac.ir**Funding information**

Research Council of Yazd University

Nanocellulose (NC) materials have some unique properties, which make them attractive as organic or inorganic supports for catalytic applications. Nanocatalysts with diameters of less than 100 nm are difficult to separate from the reaction mixture, therefore, magnetic nanoparticles (MNPs) were used as catalysts to overcome this problem. Fe₃O₄@NCs/BF_{0.2} as a green, bio-based, eco-friendly, and recyclable catalyst was synthesized and characterized using fourier-transform infrared spectroscopy (FT-IR), vibrating sample magnetometer (VSM), X-ray diffraction (XRD), X-ray fluorescence (XRF), Brunauer–Emmett–Teller (BET), field emission scanning electron microscopy (FESEM), transmission electron microscopy (TEM), and thermal gravimetric analysis (TGA) techniques. Fe₃O₄@NCs/BF_{0.2} was employed for the synthesis of 2,3-dihydro-1*H*-perimidine derivatives via a reaction of 1,8-diaminonaphthalene with various aldehydes at room temperature under solvent-free conditions. The present procedure offers several advantages including a short reaction time, excellent yields, easy separation of catalyst, and environmental friendliness.

KEY WORDS1,8-diaminonaphthalene, bio-based catalyst, Fe₃O₄@NCs/BF_{0.2}, nanocellulose, perimidine

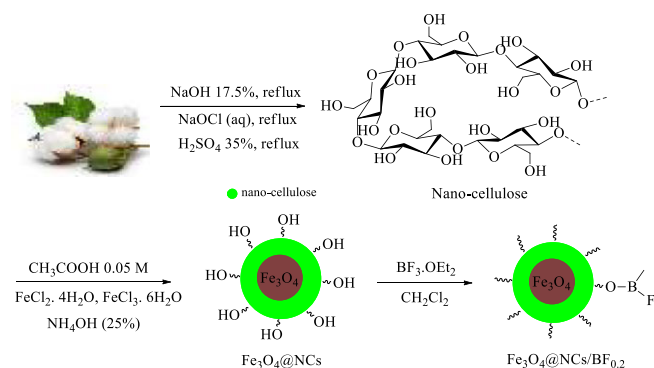
1 | INTRODUCTION

Perimidines constitute an important class of natural and non-natural products. They have attracted great attention in synthetic organic chemistry for several reasons, including biological activities, pharmacological applications such as anti-inflammatory, antibacterial, antimicrobial, antifungal, antitumor, antihypertensive, and antiviral agents.^[1–3]

A synthetic method for the preparation of perimidines is the condensation reaction of 1,8-diaminonaphthalene with various carbonyl compounds such as carboxylic acids, anhydrides, acid halides, ketones, or aldehyde reagents.^[4] These compounds have been synthesized in the presence of various catalysts, such as, FePO₄,^[5] Cu(NO₃)₂·6H₂O,^[6] nanosilica sulfuric acid,^[7] NaY zeolite,^[8] nano-CuY zeolite,^[9] *N*-bromosuccinamide,^[2] and CMK-5-SO₃H.^[10]

Cellulose has important properties such as biocompatibility, biodegradability, low toxicity,^[11] and functionalized surface.^[12,13] Nanocellulose (NC) materials have some unique properties, which make them attractive for organic or inorganic supports for catalytic applications. Nanocatalysts with diameters of less than 100 nm are difficult to separate from the reaction mixture, therefore, magnetic nanoparticles (MNPs) were used as catalysts to overcome this problem. Also MNPs in chemical synthesis offer advantages such as nontoxic, retrievable, readily accessible,^[14] low price, good stability, and easy separation by magnetic forces.^[15–18]

In this work, Fe₃O₄@nanocellulose/BF_{0.2} (Fe₃O₄@NCs/BF_{0.2}) was synthesized as a new NC-based superparamagnetic nanocatalyst. This catalyst was successfully applied to the synthesis of 2,3-dihydro-1*H*-perimidine derivatives by cyclocondensation of 1,8-diaminonaphthalene with aromatic aldehydes.



SCHEME 1 Graphical representation of $\text{Fe}_3\text{O}_4@\text{NCs}/\text{BF}_{0.2}$ preparation

2 | RESULTS AND DISCUSSION

In this work, $\text{Fe}_3\text{O}_4@\text{NCs}/\text{BF}_{0.2}$ was prepared in several steps. At first, NC was obtained from the acid hydrolysis of cotton. In this step, the free OH groups in NC were increased and could be used in the synthesis of NC-supported catalysts. $\text{Fe}_3\text{O}_4@\text{nanocellulose}$ was obtained simply through coprecipitation of ferric and ferrous ions with ammonium hydroxide in an aqueous solution containing NC. At the end, preparation of $\text{Fe}_3\text{O}_4@\text{NCs}/\text{BF}_{0.2}$ was done via mixing of $\text{Fe}_3\text{O}_4@\text{nanocellulose}$ and $\text{BF}_3 \cdot \text{OEt}_2$ at room temperature. The OH groups in the NC act as a nucleophile and B–O–C bonds were formed by the interaction between the BF_3 and the OH groups (Scheme 1).

The morphology and structure of the prepared $\text{Fe}_3\text{O}_4@\text{NCs}/\text{BF}_{0.2}$ composite were characterized through FT-IR, vibrating sample magnetometer (VSM), X-ray diffraction (XRD), XRF, Brunauer–Emmett–Teller (BET), field emission scanning electron microscopy (FESEM), transmission electron microscopy (TEM), and thermal gravimetric analysis (TGA) techniques. The FT-IR spectra of Fe_3O_4 ,

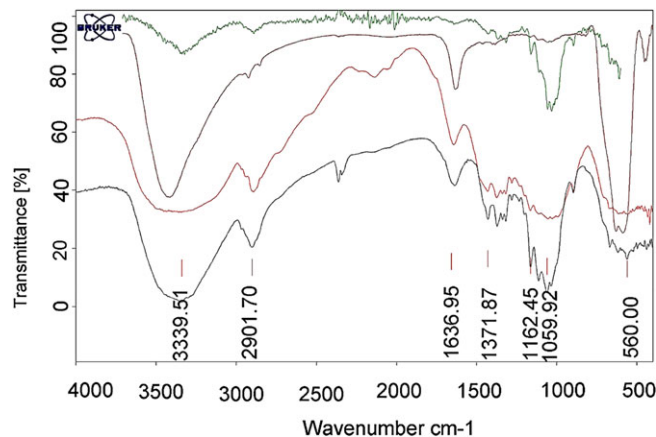


FIGURE 1 (a) Fe_3O_4 , (b) Nanocellulose, (c) $\text{Fe}_3\text{O}_4@\text{NCs}$, and (d) $\text{Fe}_3\text{O}_4@\text{NCs}/\text{BF}_{0.2}$

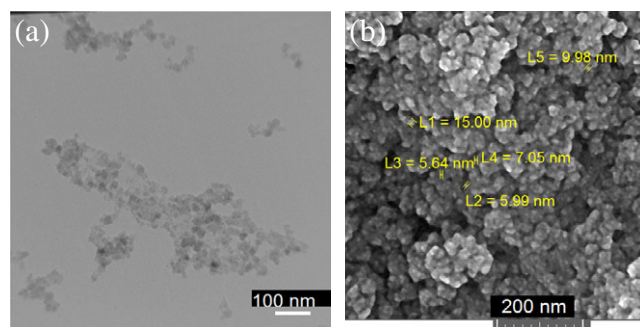


FIGURE 2 (a) TEM and (b) FESEM images of $\text{Fe}_3\text{O}_4@\text{NCs}/\text{BF}_{0.2}$

NC, $\text{Fe}_3\text{O}_4@\text{NCs}$, and $\text{Fe}_3\text{O}_4@\text{NCs}/\text{BF}_{0.2}$ are shown in Figure 1.

The FT-IR spectrum of $\text{Fe}_3\text{O}_4@\text{NCs}/\text{BF}_{0.2}$ shows the stretching vibrations of the OH group at 3334 cm^{-1} and the stretching vibrations of the C–O group appear at around 1032 and 1160 cm^{-1} . In addition to the above-mentioned bands, a broad band at 567 cm^{-1} corresponds to Fe/O stretching vibrations in the Fe_3O_4 Lattice. Figure 2 represents the FESEM and TEM images of $\text{Fe}_3\text{O}_4@\text{NCs}/\text{BF}_{0.2}$, which were used to investigate the particle size and surface morphology. This image indicates that the $\text{Fe}_3\text{O}_4@\text{NCs}/\text{BF}_{0.2}$ particles are on average below 20 nm.

The XRD patterns of Fe_3O_4 , $\text{Fe}_3\text{O}_4@\text{NCs}$, and $\text{Fe}_3\text{O}_4@\text{NCs}/\text{BF}_{0.2}$ are shown in Figure 3. According to the XRD patterns of $\text{Fe}_3\text{O}_4@\text{NCs}/\text{BF}_{0.2}$ (Figure 3a), a signal in 2θ equal to 23 confirmed the existence of cellulose in its

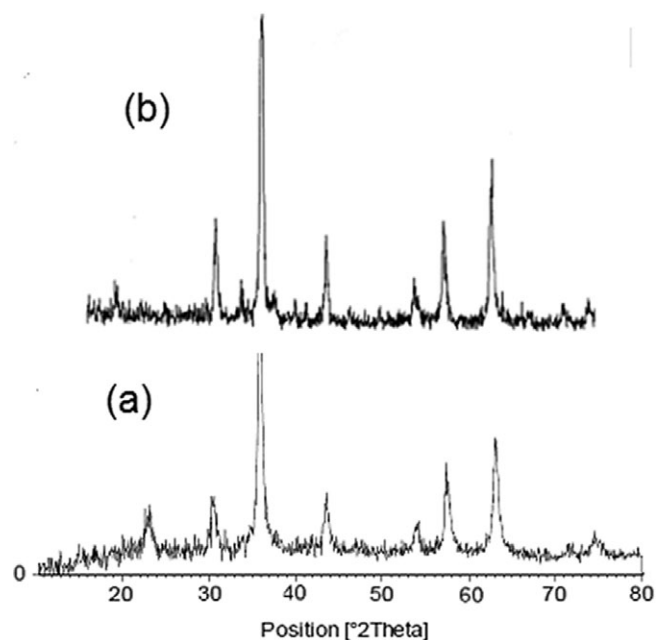


FIGURE 3 The XRD patterns of: (a) $\text{Fe}_3\text{O}_4@\text{NCs}/\text{BF}_{0.2}$, (b) Fe_3O_4

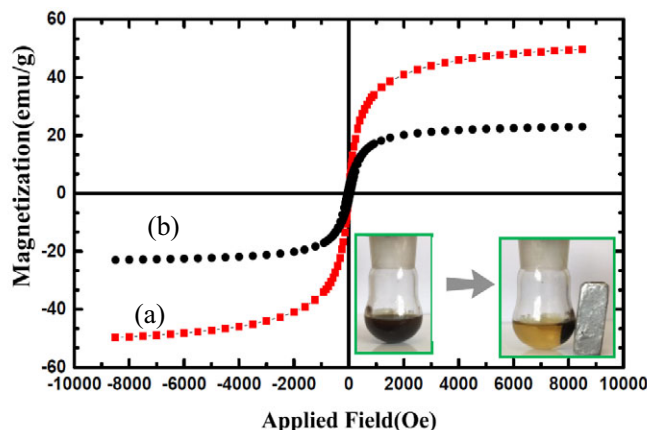


FIGURE 4 Magnetization loops of (a) Fe_3O_4 and (b) $\text{Fe}_3\text{O}_4@\text{NCs}/\text{BF}_{0.2}$

structure. The signals in $2\theta = 30, 36, 43, 54, 57$, and 63 demonstrate the existence of Fe_3O_4 .

The magnetic properties of Fe_3O_4 and $\text{Fe}_3\text{O}_4@\text{NCs}/\text{BF}_{0.2}$ were investigated at room temperature (300 K) using VSM studies (Figure 4), no hysteresis loop and no remanence were detected and also the coercivity value is zero for two samples, suggesting typical superparamagnetic property at room temperature. The amounts of saturation magnetization for Fe_3O_4 and $\text{Fe}_3\text{O}_4@\text{NCs}/\text{BF}_{0.2}$ are 50 and 23 emu/g, respectively. Despite this significant decrease, the catalyst can still be easily separated from the reaction mixture by using an external magnet.

To investigate the elemental component of $\text{Fe}_3\text{O}_4@\text{NCs}/\text{BF}_{0.2}$, XRF analysis of the catalyst was done by comparison of its kilo counts per second (KCPS) of elements in the catalyst with pure samples (NaF , H_3BO_3), (Table 1). The amounts obtained for B and F are 3.496 g (0.32 mol) and 1.112 g (0.059 mol), respectively. Thus, the B:F ratio, in the catalyst, is approximately 5:1.

The specific surface area of the catalyst was measured using the BET theory (Figure 5a). The single point surface area at $P/P_0 = 0.0685$ is $65.9890 \text{ m}^2/\text{g}$ and the BET surface area is $74.2480 \text{ m}^2/\text{g}$. The N_2 adsorption isotherm of the catalyst is depicted in Figure 5b.

TGA-DTA analysis was performed to estimate thermal stability of the $\text{Fe}_3\text{O}_4@\text{NCs}/\text{BF}_{0.2}$ in the temperature range of $26\text{--}814^\circ\text{C}$ (Figure 6). The TGA curve illustrates three stages of weight loss. The first weight loss at 93°C (5% weight loss) is related to the removal of moisture from the

TABLE 1 XRF analysis of the catalyst and pure samples

Elemental component	$\text{Fe}_3\text{O}_4@\text{NCs}/\text{BF}_{0.2}$			H_3BO_3		NaF	
	B%	F%	KCPS	B%	KCPS	F%	KCPS
B	3.496	—	0.5	17.48	2.5	—	—
F	—	1.112	1	—	—	45.25	40.7

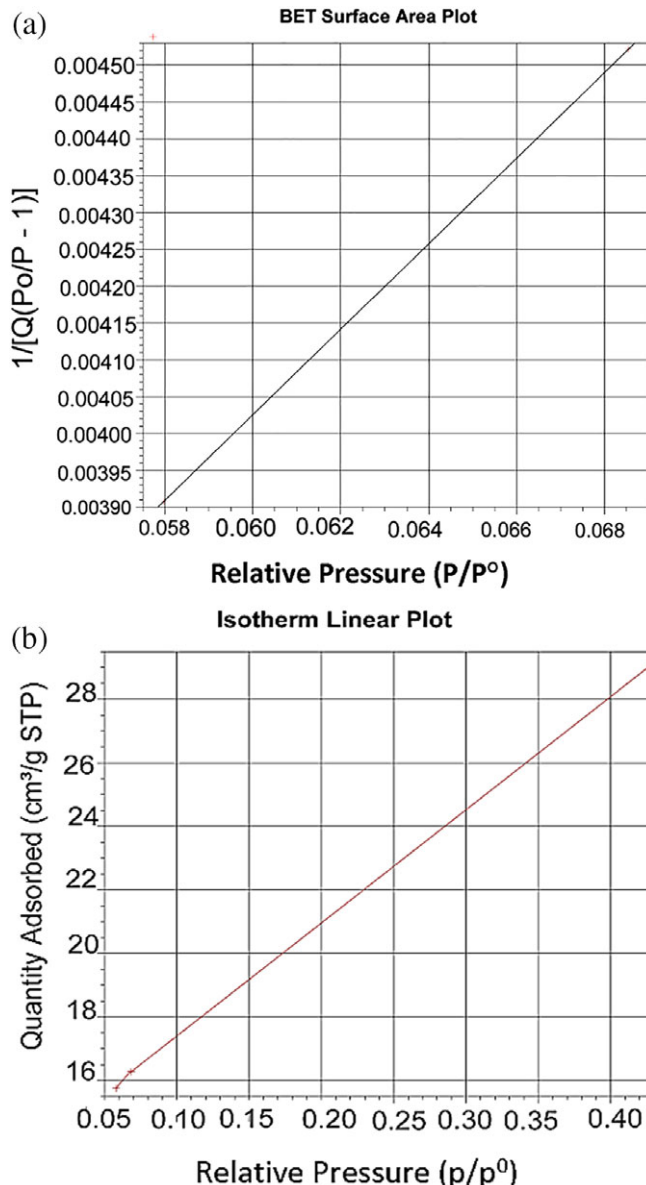


FIGURE 5 (a) BET of $\text{Fe}_3\text{O}_4@\text{NCs}/\text{BF}_{0.2}$ and (b) nitrogen adsorption isotherms of $\text{Fe}_3\text{O}_4@\text{NCs}/\text{BF}_{0.2}$

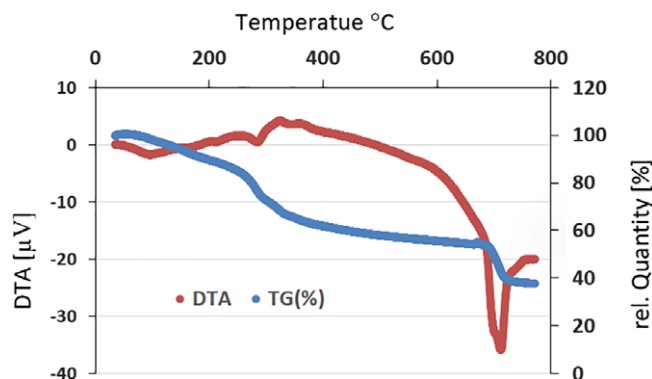


FIGURE 6 Thermal gravimetric analysis patterns of $\text{Fe}_3\text{O}_4@\text{NCs}/\text{BF}_{0.2}$

catalyst. The next weight loss (52%) appears in the range of 100–670°C and is related to the decomposition of cellulosic units in the nanocomposite. Finally, the main weight loss (6%) is observed in the range of 670–700°C.

3 | EXPERIMENTAL

3.1 | Materials and methods

All compounds were purchased from Aldrich, Merck, and Fluka chemical companies. NCs and Fe₃O₄@nanocellulose (Fe₃O₄@NCs) were synthesized *via* our previously reported methods.^[16–19] FT-IR spectra were run on a Bruker, Equinox 55 spectrometer. A Bruker (DRX-400 Avance) NMR was used to record the ¹H NMR and ¹³C NMR spectra. The XRD pattern was obtained using a Philips Xpert MPD diffract meter equipped with a Cu K α anode ($k = 1.54 \text{ \AA}$) in the 2θ range from 10 to 80°. XRF analysis was done using a Bruker, S4 Explorer instrument. VSM measurements were performed using a VSM (Meghnatis Daghigh Kavir Co. Kashan, Iran), a refrigerated centrifuge (Appendorf Centrifuge 5417R) was used for the preparation of NC. Melting points were determined using a Buchi melting point B-540 B.V.CHI apparatus. The FESEM image was obtained on a Mira 3-XMU. The TEM image was obtained using a Philips CM120 with a LaB6 cathode and an accelerating voltage of 120 kV. Quantitative elemental information (EDS) of Fe₃O₄@NCs/BF_{0.2} was obtained using an EDS instrument and Phenom pro X. TGA was conducted using a “STA 504” instrument. The BET surface area of the catalyst was analyzed using a Micromeritics, Tristar II 3020 analyzer.

3.2 | Preparation of Fe₃O₄@NCs/BF_{0.2}

In a beaker, 10 mL of dichloromethane was added to a Fe₃O₄@NCs (0.5 g) and stirred at room temperature. Then, 0.5 mL BF₃.OEt₂ was added dropwise to a mixture and stirred for 1 hr at room temperature. After this, the mixture was filtered, washed with dichloromethane, dried at room temperature, and the Fe₃O₄@NCs/BF_{0.2} catalyst was obtained.

3.3 | General procedure for synthesis of 2,3-dihydro-1H-perimidines

Fe₃O₄@NCs/BF_{0.2} (0.03 g) as a catalyst was added to a mixture of aromatic aldehyde (1.0 mmol) and 1,8-diaminonaphthalene (1.0 mmol). The mixture was stirred at room temperature. After completion of the reaction (monitored by TLC, *n*-hexane:diethylether [70:30]), the reaction mixture was dissolved in acetone and the catalyst was

separated using an external magnet. Then, by adding water to the residue, the pure products were obtained.

3.4 | Selected spectral data

3.4.1 | 2-(4-Methoxyphenyl)-2, 3-dihydro-1H-perimidine (3b)

FTIR (ATR) $\bar{\nu}/\text{cm}^{-1}$ 3,362, 3,041, 1,592, 1,406, 1,239, 1,023, and 811; ¹HNMR (DMSO-d₆, 400 MHz): $\delta = 3.76$ (s, 3H), 5.28 (s, 1H), 6.46 (d, $J = 7.2 \text{ Hz}$, 2H), 6.65 (s, 2H), 6.96 (m, $J = 6.8 \text{ Hz}$, 4H), 7.12 (t, $J = 8.0 \text{ Hz}$, 2H), and 7.52 (d, $J = 7.2 \text{ Hz}$, 2H).

3.4.2 | 2-(2, 4-Dimethoxyphenyl)-2, 3-dihydro-1H-perimidine (3c)

FTIR (ATR) $\bar{\nu}/\text{cm}^{-1}$ 3,358, 3,048, 1,597, 1,417, 1,265, and 1,032; ¹HNMR (DMSO-d₆, 400 MHz): $\delta = 3.33$ (s, 1H), 3.76 (s, 3H), 3.81 (s, 3H), 5.60 (s, 1H), 6.44 (s, 1H), 6.46 (d, $J = 7.2 \text{ Hz}$, 2H), 6.55 (d, $J = 6.8 \text{ Hz}$, 1H), 6.60 (s, 1H), 6.94 (d, $J = 7.6 \text{ Hz}$, 2H), 7.12 (t, $J = 8.0 \text{ Hz}$, 2H), and 7.45 (d, $J = 8.4 \text{ Hz}$, 1H).

3.4.3 | 2-(4-Dimethylaminophenyl)-2, 3-dihydro-1H-perimidine (3d)

FTIR (ATR) $\bar{\nu}/\text{cm}^{-1}$ 3,334, 3,042, 1,590, 1,410, and 809; ¹HNMR (DMSO-d₆, 400 MHz): $\delta = 2.89$ (s, 6H), 3.34 (s, 1H), 5.21 (s, 1H), 6.45 (d, $J = 7.2 \text{ Hz}$, 2H), 6.57 (s, 1H), 6.75 (d, $J = 6.8 \text{ Hz}$, 2H), 6.93 (d, $J = 8 \text{ Hz}$, 2H), 7.11 (t, $J = 8 \text{ Hz}$, 2H), and 7.39 (d, $J = 7.2 \text{ Hz}$, 2H).

3.4.4 | 2-(3, 4-Dimethoxyphenyl)-2, 3-dihydro-1H-perimidine (3e)

FTIR (ATR) $\bar{\nu}/\text{cm}^{-1}$ 3,347, 3,048, 1,593, 1,460, 1,261, 1,019, and 859, 811; ¹HNMR (DMSO-d₆, 400 MHz): $\delta = 3.75$ (s, 3H), 3.76 (s, 3H), 5.27 (s, 1H), 6.47 (d, $J = 7.2 \text{ Hz}$, 2H), 6.66 (s, 1H), 6.97–7.15 (m, 7H), and 7.2 (s, 1H).

3.4.5 | 2-(4-Carboxyphenyl)-2, 3-dihydro-1H-perimidine (3f)

FTIR (ATR) $\bar{\nu}/\text{cm}^{-1}$ 3,343, 3,051, 1,687, 1,592, 1,499, and 814; ¹HNMR (DMSO-d₆, 400 MHz): $\delta = 3.99$ (s, 1H), 5.42 (s, 1H), 6.49 (d, $J = 7.2 \text{ Hz}$, 2H), 6.85 (s, 1H), 6.98 (d, $J = 8 \text{ Hz}$, 2H), 7.16 (t, $J = 7.6 \text{ Hz}$, 2H), 7.62 (d, $J = 8.4 \text{ Hz}$, 2H), 7.98 (d, $J = 8 \text{ Hz}$, 2H), and 13 (s, 1H).

3.4.6 | 2-(4-Chlorophenyl)-2, 3-dihydro-1H-perimidine (3g)

FTIR (ATR) $\bar{\nu}/\text{cm}^{-1}$ 3,387, 3,036, 1,595, 1,483, 1,086, and 812; ¹HNMR (DMSO-d₆, 400 MHz): $\delta = 5.35$ (s, 1H), 6.47

(d, $J = 6.8$, 2H), 6.79 (s, 1H), 6.97 (d, $J = 8.0$ Hz, 2H), 7.13 (t, $J = 7.6$ Hz, 2H), 7.16 (s, 1H), 7.48 (d, $J = 7.9$ Hz, 2H), and 7.60 (d, $J = 7.9$ Hz, 2H).

3.4.7 | 2-(2-Nitrophenyl)-2, 3-dihydro-1H-perimidine (3h)

FTIR (ATR) $\bar{\nu}$ /cm⁻¹ 3,365, 3,068, 1,597, 1,511, 1,345, and 1,411; ¹HNMR (DMSO-d₆, 400 MHz): $\delta = 3.34$ (s, 1H), 5.79 (s, 1H), 6.51 (d, $J = 7.2$, 2H), 6.8 (s, 1H), 7.01 (d, $J = 8.4$ Hz, 2H), 7.16 (t, $J = 8.0$ Hz, 1H), 7.61 (t, $J = 8.0$ Hz, 2H), 7.75 (t, $J = 6.8$ Hz, 1H), 7.89 (d, $J = 8.0$ Hz, 1H), and 8.02 (d, $J = 8.0$ Hz, 1H).

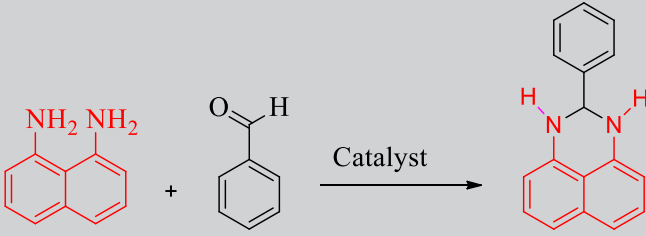
3.4.8 | 2-(3-Nitrophenyl)-2, 3-dihydro-1H-perimidine (3i)

FTIR (ATR) $\bar{\nu}$ /cm⁻¹ 3,343, 3,044, 1,593, 1,519, 1,343, and 1,412; ¹HNMR (DMSO-d₆, 400 MHz): $\delta = 5.6$ (s, 1H), 6.50 (d, $J = 7.2$ Hz, 2H), 6.98 (s, 1H), 7.01 (d, $J = 8.4$ Hz, 2H), 7.15 (t, $J = 7.6$ Hz, 2H), 7.62 (t, $J = 8.0$ Hz, 1H), 7.97 (d, $J = 7.6$ Hz, 1H), 8.18 (d, $J = 6.8$ Hz, 1H), and 8.37 (s, 1H).

3.4.9 | 2-(4-Nitrophenyl)-2, 3-dihydro-1H-perimidine (3j)

FTIR (ATR) $\bar{\nu}$ /cm⁻¹ 3,365, 3,068, 1,595, 1,410, 1,511, 1,343, and 811; ¹HNMR (DMSO-d₆, 400 MHz): $\delta = 3.34$

TABLE 2 The reaction of 1,8-diaminonaphthalene (1.0 mmol) and benzaldehyde (1.0 mmol), in the presence of Fe₃O₄@NCs/BF_{0.2} under various conditions



Entry	Catalyst (g)	Condition	Solvent	Time (min)	Yield (%) ^a
1	—	r.t. ^b	—	20	53
2	Fe ₃ O ₄ (0.06)	r.t. ^b	—	20	64
3	Fe ₃ O ₄ @NCs (0.06)	r.t. ^b	—	20	50
4	Fe ₃ O ₄ @NCs/BF _{0.2} (0.015)	r.t. ^b	—	20	82
5	Fe ₃ O ₄ @NCs/BF _{0.2} (0.03)	r.t. ^b	—	5	98
6	Fe ₃ O ₄ @NCs/BF _{0.2} (0.05)	r.t. ^b	—	20	94
7	Fe ₃ O ₄ @NCs/BF _{0.2} (0.03)	Microwave	—	5	66
8	Fe ₃ O ₄ @NCs/BF _{0.2} (0.03)	Mixer mill	—	5	70
9	Fe ₃ O ₄ @NCs/BF _{0.2} (0.03)	Ultrasound bath	—	5	93
10	Fe ₃ O ₄ @NCs/BF _{0.2} (0.03)	Ultrasound	EtOH	5	45
11	Fe ₃ O ₄ @NCs/BF _{0.2} (0.03)	Ultrasound	H ₂ O	5	71
12	Fe ₃ O ₄ @NCs/BF _{0.2} (0.03)	Ultrasound	H ₂ O:EtOH (1:1)	5	80
13	Fe ₃ O ₄ @NCs/BF _{0.2} (0.03)	Ultrasound	PEG 400	5	83
14	Fe ₃ O ₄ @NCs/BF _{0.2} (0.03)	Ultrasound	Acetone	5	81
15	Fe ₃ O ₄ @NCs/BF _{0.2} (0.03)	Ultrasound	MeOH	5	81
16	Fe ₃ O ₄ @NCs/BF _{0.2} (0.03)	Ultrasound	CH ₂ Cl ₂	5	79
17	Fe ₃ O ₄ @NCs/BF _{0.2} (0.03)	r.t. ^b	H ₂ O	180	40
18	Fe ₃ O ₄ @NCs/BF _{0.2} (0.03)	r.t. ^b	EtOH	180	58
19	Fe ₃ O ₄ @NCs/BF _{0.2} (0.03)	r.t. ^b	H ₂ O:EtOH (1:1)	180	25

^aIsolated yield.

^bRoom temperature.

(s, 1H), 5.48 (s, 1H), 6.49 (d, $J = 7.2$ Hz, 2H), 6.98 (d, $J = 8.4$ Hz, 3H), 7.15 (t, 2H, $J = 7.6$ Hz), 7.78 (d, $J = 8.4$ Hz, 2H), and 8.21 (d, $J = 8.8$ Hz, 2H).

3.4.10 | 2-(2, 3-Dichlorophenyl)-2, 3-dihydro-1H-perimidine (3k)

FTIR (ATR) $\bar{\nu}/\text{cm}^{-1}$: 13,347, 3,047, 1,595, 1,404, 1,039, 751, and 645; ^1H NMR (DMSO- d_6 , 400 MHz): $\delta = 3.35$ (s, 1H), 5.77 (s, 1H), 6.5 (d, $J = 6.8$ Hz, 2H), 6.83 (s, 1H), 7.02 (d, $J = 8.0$ Hz, 2H), 7.17 (t, $J = 7.2$ Hz, 2H), 7.43 (t, $J = 7.6$ Hz, 1H), and 7.67 (d, $J = 6.8$ Hz, 2H).

3.4.11 | 2-(2, 3-Dimethoxyphenyl)-2, 3-dihydro-1H-perimidine (3l)

FTIR (ATR) $\bar{\nu}/\text{cm}^{-1}$: 13,355, 3,048, 1,595, 1,417, 1,260, 1,060, 751, and 638; ^1H NMR (DMSO- d_6 , 400 MHz): $\delta = 3.79$ (s, 3H), 3.82 (s, 3H), 5.65 (s, 1H), 6.48 (d, $J = 7.2$ Hz, 2H), 6.55 (s, 1H), and 6.96–7.16(m, 9H).

3.5 | Catalytic activity of $\text{Fe}_3\text{O}_4@\text{NCs}/\text{BF}_{0.2}$

After characterization of the catalyst, the catalytic activity of $\text{Fe}_3\text{O}_4@\text{NCs}/\text{BF}_{0.2}$ was investigated for the synthesis of 2,3-dihydro-1H-perimidine derivatives. 2-phenyl-2,3-dihydro-1H-perimidine was synthesized via condensation of 1,8-diaminonaphthalene (1.0 mmol) with benzaldehyde (1.0 mmol) as model reaction. To optimize the reaction conditions, the effects of several parameters such as catalyst amount, solvent, and reaction time were studied (Table 2). According to Table 2, the best condition for the reaction is a solvent-free condition using 0.03 g of $\text{Fe}_3\text{O}_4@\text{NCs}/\text{BF}_{0.2}$ as an efficient catalyst at room temperature (Table 2, entry 21).

Based on optimal reaction conditions, 2,3-dihydro-1H-perimidine derivatives were synthesized using the two-component condensation of various aldehydes (1.0 mmol) and 1,8-diaminonaphthalene (1.0 mmol) (Table 3). All synthesized compounds were identified using melting point, FT-IR, ^1H -NMR, and ^{13}C -NMR spectroscopy.

TABLE 3 Synthesis of 2,3-dihydro-1H-perimidine derivatives (III_{a–l}) in the presence of $\text{Fe}_3\text{O}_4@\text{NCs}/\text{BF}_{0.2}$ ^a

(1)
(2)
(3)

					M.P.	
Entry	R	Product	Time (min)	Yield (%) ^b	Found	Reported [ref.]
1	H	3a	5	98	101–103	103–105 ^[20]
2	4-OMe	3b	15	91	156–158	160–162 ^[7]
3	2,4-(OMe) ₂	3c	15	75	205–207	— ^[21]
4	4-NMe ₂	3d	15	86	50–52	51–53 ^[20]
5	3,4-(OMe) ₂	3e	15	92	202–203	206–207 ^[7]
6	4-COOH	3f	10	99	200–202	— ^[21]
7	4-Cl	3g	10	96	153–155	154–156 ^[20]
8	2-NO ₂	3h	12	94	157–159	158–160 ^[5]
9	3-NO ₂	3i	10	96	189–191	188–190 ^[5]
10	4-NO ₂	3j	10	99	199–201	201–202 ^[9]
11	2,3-(Cl) ₂	3k	15	88	165–167	— ^[21]
12	2,3-(OMe) ₂	3l	20	85	102–103	— ^[21]

^aReaction conditions: 1,8-diaminonaphthalene (1.0 mmol), aldehyde (1.0 mmol), and $\text{Fe}_3\text{O}_4@\text{NCs}/\text{BF}_{0.2}$ (0.03 g).

^bIsolated yield.

TABLE 4 Comparison of the $\text{Fe}_3\text{O}_4@\text{NCs}/\text{BF}_{0.2}$ catalyst with reported catalysts for the synthesis of 2,3-dihydro-1*H*-perimidine derivatives

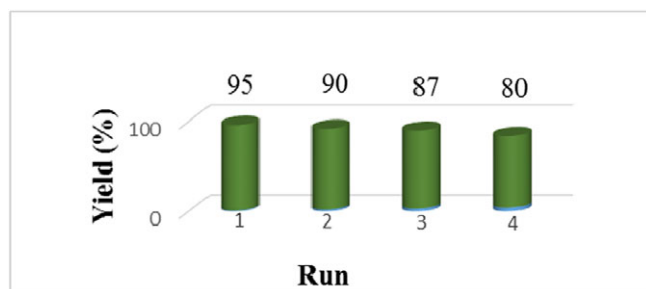
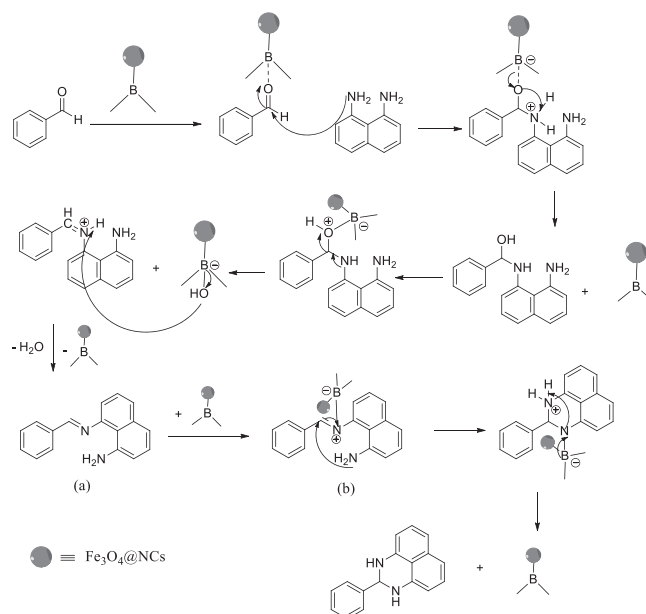
Entry	Catalyst	Condition	Solvent	Time	Yield (%)	Ref.
1	Acetic acid (a few drops)	r.t.	EtOH	24 hr	52	[22]
2	NSSA ^a (2 mg)	r.t.	EtOH	50 min	84	[7]
3	$\text{Cu}(\text{NO}_3)_2 \cdot 6\text{H}_2\text{O}$ (5 mol%)	r.t.	EtOH	10 min	83	[6]
4	CuY zeolite (0.002 g)	r.t.	EtOH	25 min	81	[9]
5	FePO_4 (0.01 g)	r.t.	EtOH	12 hr	80	[5]
6	MNPs-TBSA ^b (20 mg)	50°C	EtOH/ H_2O (1:1)	25 min	90	[22]
7	Iodine (7 mol%)	r.t.	EtOH	40 min	84	[23]
8	NaY zeolite (0.20 g)	r.t.	EtOH	45 hr	70	[8]
9	$\text{Yb}(\text{OTf})_3$ (0.1 eq.)	r.t.	Acetonitrile	1 hr	88	[24]
10	$\text{Na}_2\text{S}_2\text{O}_5$ (1.9 g)	Reflux	EtOH/ H_2O (1:1)	1 hr	95	[25]
11	$\text{Fe}_3\text{O}_4@\text{NCs}/\text{BF}_{0.2}$ (0.03 g)	—	—	5 min	98	This work

^aNanosilica sulfuric acid.^bTriazinediyl bis-sulfamic acid-grafted magnetite nanoparticles.

The comparison of data of the efficiency of $\text{Fe}_3\text{O}_4@\text{NCs}/\text{BF}_{0.2}$ with that of other reported catalysts for the synthesis of 2-phenyl-2,3-dihydro-1*H*-perimidines is indicated in Table 4. We have observed good and high yields of products under very mild and green conditions using $\text{Fe}_3\text{O}_4@\text{NCs}/\text{BF}_{0.2}$. The results show that with $\text{Fe}_3\text{O}_4@\text{NCs}/\text{BF}_{0.2}$, 2,3-dihydro-1*H*-perimidine derivatives can be synthesized as 2-phenyl-2,3-dihydro-1*H*-perimidines in a shorter time and under green conditions with higher yields. Other advantages of $\text{Fe}_3\text{O}_4@\text{NCs}/\text{BF}_{0.2}$ as a catalyst are environmental friendliness, biodegradation, reusability, and easy separation with an external magnet.

The reusability of the catalyst was also investigated on the model reaction. The magnetic catalyst was separated using an external magnet, washed with acetone, dried at room temperature, and reused for subsequent reactions. It was observed that the recovered biocatalyst could be used at least four times with little decrease in its catalytic activity (Figure 7).

The proposed mechanism for the synthesis of 2-phenyl-2,3-dihydro-1*H*-perimidine in the presence of $\text{Fe}_3\text{O}_4@\text{NCs}/\text{BF}_{0.2}$ is shown in Scheme 2. At first, $\text{Fe}_3\text{O}_4@\text{NCs}/\text{BF}_{0.2}$ as Lewis acid attacked the carbonyl group of aldehyde. Then,

**FIGURE 7** Catalyst recycling experiments**SCHEME 2** Proposed mechanism for the synthesis of 2-phenyl-2,3-dihydro-1*H*-perimidines

nucleophilic attack of 1,8-diaminonaphthalene on activated aldehyde generated imine intermediate (a). The nucleophilic attack of the second amino group on the activated imine intermediate afforded intermediate (b). Finally, with the transfer of proton, the product is produced.

4 | CONCLUSIONS

In summary, $\text{Fe}_3\text{O}_4@\text{NCs}/\text{BF}_{0.2}$ was successfully synthesized and characterized. It was applied for the synthesis of

of 2,3-dihydro-1*H*-perimidine derivatives through the reaction of 1,8-diaminonaphthalene and aromatic aldehydes under solvent-free conditions at room temperature. This method offers several advantages including easy work-up, excellent yields, short reaction time, and environmental friendliness.

ACKNOWLEDGMENTS

The Research Council of Yazd University is gratefully acknowledged for the financial support for this work.

ORCID

Bi Bi Fatemeh Mirjalili  <https://orcid.org/0000-0002-6588-4041>

REFERENCES

- [1] T. A. Farghaly, E. M. Abbas, *Molecules* **2014**, *19*, 740.
- [2] M. H. Krishna, P. Thriveni, *J. Chem. Pharm. Res.* **2016**, *8*, 809.
- [3] D. R. Panchasara, S. Pande, *E-J. Chem.* **2009**, *6*, 91.
- [4] M. M. Belmonte, E. C. Escudero-Adán, J. Benet-Buchholz, R. M. Haak, A. W. Kleij, *Eur. J. Org. Chem.* **2010**, *25*, 4823.
- [5] F. K. Behbahani, F. M. Golchin, *J. Taibah Univ. Sci.* **2017**, *11*, 85.
- [6] A. Mobinikhaledi, P. J. Steel, *Synth. React. Inorg. Met. Org. Chem.* **2009**, *39*, 133.
- [7] A. Mobinikhaledi, H. Moghanian, F. Sasani, *Int. J. Green Nanotechnol. Phys. Chem.* **2010**, *2*, 47.
- [8] A. Mobinikhaledi, N. Forughifar, N. Bassaki, *Turk. J. Chem.* **2009**, *33*, 555.
- [9] M. Kalhor, N. Khodaparast, *Res. Chem. Intermed.* **2015**, *41*, 3235.
- [10] H. Alinezhad, M. Zare, *J. Chil. Chem. Soc.* **2013**, *58*, 1840.
- [11] M. Jorfi, E. J. Foster, *J. Appl. Polym. Sci.* **2015**, *132*, 41719.
- [12] X. An, Y. Long, Y. Ni, *Carbohydr. Polym.* **2017**, *156*, 253.
- [13] H. Wei, K. Rodriguez, S. Renneckar, P. J. Vikesland, *Environ. Sci. Nano.* **2014**, *1*, 302.
- [14] N. Azgomi, M. Mokhtary, *J. Mol. Catal. A: Chem.* **2015**, *398*, 58.
- [15] X. Zheng, S. Luo, L. Zhang, J. P. Cheng, *Green Chem.* **2009**, *11*, 455.
- [16] S. Azad, B. F. Mirjalili, *RSC Adv.* **2016**, *6*, 96928.
- [17] N. Salehi, B. F. Mirjalili, *RSC Adv.* **2017**, *7*, 30303.
- [18] S. Azad, B. F. Mirjalili, *Mol. Divers* **2018** in press.
- [19] B. F. Mirjalili, F. Aref, *Res. Chem. Intermed.* **2018**, *44*, 4519.
- [20] M. A. Bodaghifard, S. A. sadbegi, Z. Bahrani, *J. Iran. Chem. Soc.* **2017**, *14*, 365.
- [21] A. Bamoniri, B. F. Mirjalili, S. Saleh, *RSC Adv.* **2018**, *8*, 6178.
- [22] K. M. Salih, H. Azeez, *J. Res. Pharm. Biotechnol.* **2014**, *5*, 1.
- [23] A. Mobinikhaledi, F. Sasani, A. Hamta, S. M. Shariatzadeh, *Bulg. Chem. Commun.* **2013**, *45*, 353.
- [24] C. K. Wu, T. J. Liou, H. Y. Wei, P. S. Tsai, D. Y. Yang, *Tetrahedron* **2014**, *70*, 8219.
- [25] A. Maquestiau, L. Berte, A. Mayence, J. J. V. Eynde, *Synth. Commun.* **1991**, *21*, 2171.

SUPPORTING INFORMATION

Additional supporting information may be found online in the Supporting Information section at the end of this article.

How to cite this article: Mirjalili BBF, Imani M. Fe₃O₄@NCs/BF_{0.2}: A magnetic bio-based nanocatalyst for the synthesis of 2,3-dihydro-1*H*-perimidines. *J Chin Chem Soc.* 2019;1–8. <https://doi.org/10.1002/jccs.201900004>